



HAL
open science

Pole Arcs Optimization of Vernier Reluctance Motors Supplied with Square Wave Current

Bernard Multon, Sami Hassine, Jean-Yves Le Chenadec

► **To cite this version:**

Bernard Multon, Sami Hassine, Jean-Yves Le Chenadec. Pole Arcs Optimization of Vernier Reluctance Motors Supplied with Square Wave Current. *Electric Machines and Power Systems*, 1993, 21, pp.695-709. hal-00673915

HAL Id: hal-00673915

<https://hal.science/hal-00673915>

Submitted on 24 Feb 2012

HAL is a multi-disciplinary open access archive for the deposit and dissemination of scientific research documents, whether they are published or not. The documents may come from teaching and research institutions in France or abroad, or from public or private research centers.

L'archive ouverte pluridisciplinaire **HAL**, est destinée au dépôt et à la diffusion de documents scientifiques de niveau recherche, publiés ou non, émanant des établissements d'enseignement et de recherche français ou étrangers, des laboratoires publics ou privés.

POLE ARCS OPTIMIZATION OF VERNIER RELUCTANCE MOTORS SUPPLIED WITH SQUARE WAVE CURRENT

B. MULTON, S. HASSINE, AND J. Y. LE CHENADEC

L.E.Si.R. (Laboratoire d'Electricité Signaux et Robotique)

URA CNRS D1375

Ecole Normale Supérieure de Cachan

61, av. du President Wilson

F 94235 Cachan Cédex, France

Abstract : To maximize their performances, it is profitable to supply vernier reluctance motors (V.R.Ms.) with square wave current, but the converter has to switch this current successively into each inductive phase. This raises problems at high speeds. To obtain a high base speed, therefore a high power, we proposed to optimize pole arcs which have a highly significant importance on the permeance wave of V.R.Ms. The variation range of the angles is restricted by certain conditions, but within these limits optimization is possible. All dimensional parameters were taken into account and used to calculate average torque in linear as well as in saturated mode. We neglected the influence of mutual coupling between phases and this hypothesis was justified by results obtained through measurements. Though we used a model with linearized segments to minimize the number of parameters, the same method can be applied to other more accurate models. A V.R.M. with 6-4 structure was designed and realized ; it allowed validation of our theoretical model.

NOMENCLATURE

k_F	:	stack factor.
l	:	stack length.
n	:	number of turns for one phase.
n_i	:	amperes-turns.
N_s, N_r	:	number of teeth of stator, of rotor.
q	:	number of phases.
$\langle T \rangle$:	average torque.

U_{Pmax1}	:	maximal positive voltage.
U_{Nmax1}	:	maximal negative voltage.
$\alpha^\circ, \beta^\circ$:	pole pitches and arcs (radians or degrees).
β_{α}, β_r	:	reduced pole arcs.
φ	:	flux in magnetic circuit.
θ	:	electric angle.
$D\theta_p$:	permeance variation angle.
θ_{po}, θ_{pc}	:	opposition and conjunction angles.
ω	:	electric angular frequency (rad/s).
Ω	:	rotation (mechanical) angular speed.
Ω_b	:	base speed.

1- INTRODUCTION - MOTOR MODEL

Reluctance motors are promising in low cost appliances (automotive, domestic ...) as well as in high performance drives /1, 2, 3/. As these motors are supplied by static converters, the price of a complete drive is dependent on both motor and converter. Therefore the whole motor-converter set has to be optimized.

To maximize average torque-copper losses ratio, a supply with square wave current makes it possible to approach the optimal value /4/. However reluctance motor phases are inductive and, to inject pseudo-square currents, high switching voltage is required. It is also possible to reduce the number of turns per phase, but with the same voltage and when keeping the same torque, the current in the coil and in the converter switches is higher. As the sizing power of the converter increases or its size power ratio degrades, the ideal supply is square wave voltage /5, 6/.

A phase is characterized with its flux φ curves which are dependent on amperes-turns ni and electric angle θ . Figure 1 shows these curves and their linearization ; it is profitable to use the flux differential because it represents the instantaneous torque shape. The given values concern a V.R.M. 6-4 whose dimensions are shown in figure 2.

We defined the elements of the linearized model as follows :

- permeances in aligned position (or conjunction $\theta = \pi$) \mathcal{P}_c in non saturated zone and \mathcal{P}_s slope in saturated zone, and \mathcal{P}_o in unaligned position (or opposition $\theta = 0$), assuming there is no saturation for this angle;

- saturation amperes-turns nI_s ;

- characteristic angles of permeance wave : θ_{po} (flat opposition), $D\theta_p$ (linear variation) and θ_{pc} (flat conjunction). So, they respect the following condition :

$$\theta_{po} + 2.D\theta_p + \theta_{pc} = 2\pi \tag{1.1}$$

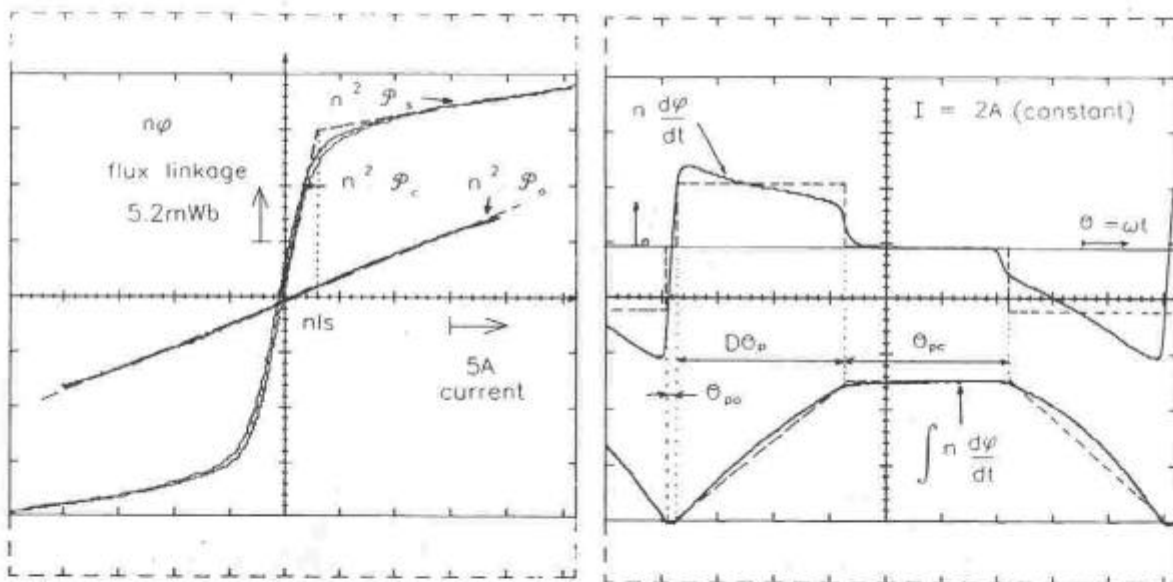


Figure -1-

Fundamental characteristic curves for one V.R.M. phase
 - - - - linearized model

These parameters can be linked to the dimensions of the magnetic circuit. Basic dimensional parameters are given in figure 2. To design tooth width, we chose to use pole arc - pole pitch ratio because it makes it easier to take into account winding problems in motor optimization /7/. Angular parameters are defined as follows :

- α_s° and α_r° are stator and rotor pole pitches :

$$\alpha_s^\circ = \frac{2\pi}{N_s} \quad \text{and} \quad \alpha_r^\circ = \frac{2\pi}{N_r} \tag{1.2}$$

(N_s and N_r are the numbers of stator and rotor teeth)

- β_s° and β_r° are stator and rotor pole arcs and we defined reduced pole arcs as follows :

$$\beta_s = \frac{\beta_s^\circ}{\alpha_s^\circ} \quad \text{and} \quad \beta_r = \frac{\beta_r^\circ}{\alpha_r^\circ} \quad [1.3]$$

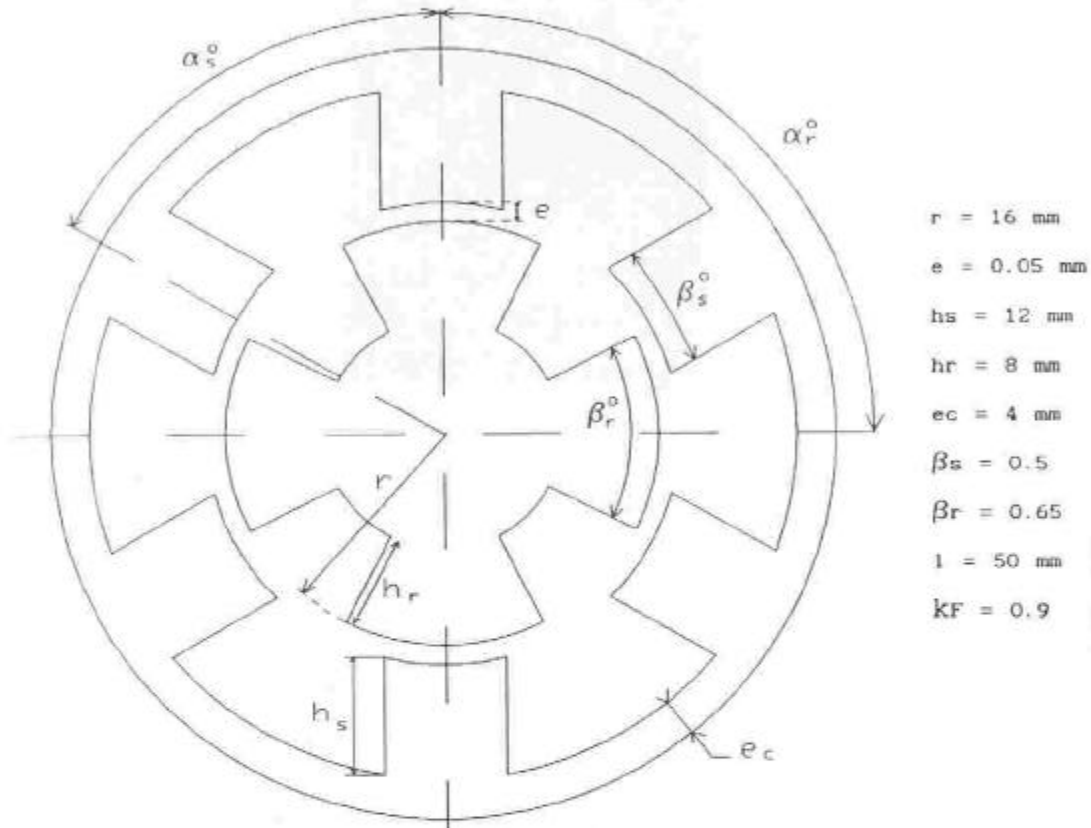


Figure -2-

Dimensional parameters of magnetic circuit

The principle of current square supply will be found in figure 3. Average torque $\langle T \rangle$ is calculated from converted energy per stroke W . This energy is equal to the area defined by the path of point (φ, ni) . So :

$$\langle T \rangle = q \cdot \frac{N_r}{2\pi} \cdot W \quad [1.4]$$

If current keeps a constant value during angle $D\theta_p$ and if it is switched within interval θ_{p0} when rising and interval θ_{pc} when falling (in motor mode and vice versa in regenerating mode), converted energy is :

$$- nIM \leq nI_s \quad W = \frac{\mathcal{P}_c - \mathcal{P}_0}{2} \cdot (nIM)^2 \quad [1.5]$$

$$- nIM > nI_s \quad W = \frac{1}{2} \left[(\mathcal{P}_c - \mathcal{P}_0) \cdot (nIM)^2 - (\mathcal{P}_c - \mathcal{P}_s)(nIM - nI_s)^2 \right]$$

[1.6]

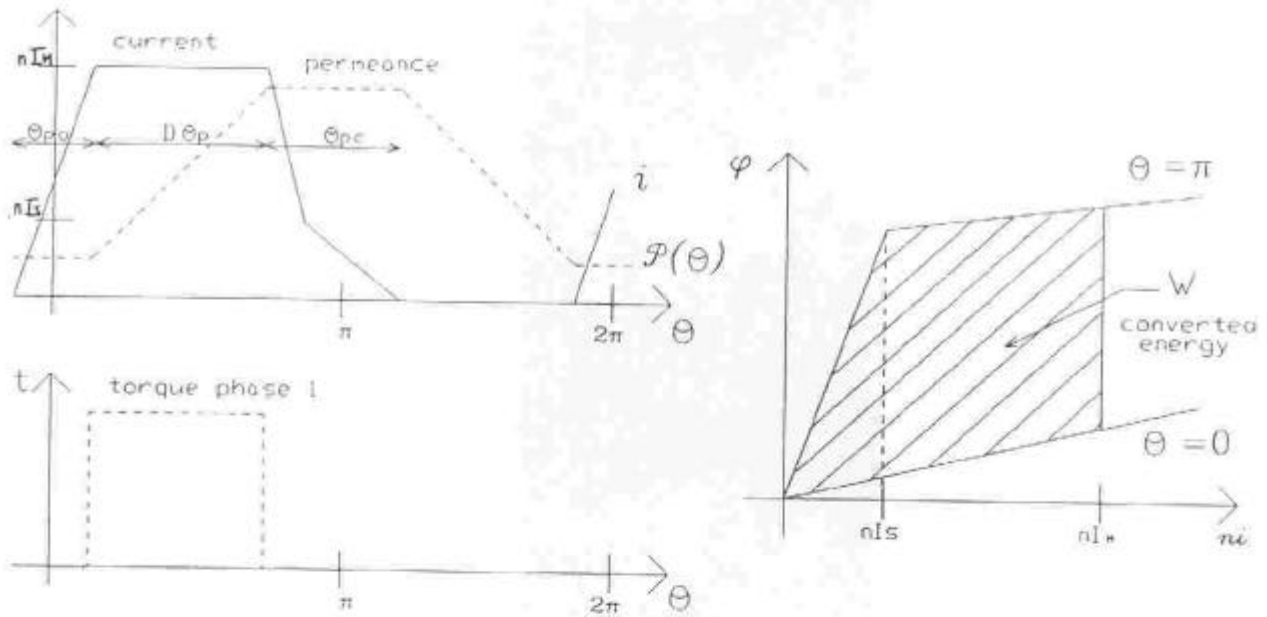


Figure -3-

Square wave current supply and energy cycle

2- RELATIONS BETWEEN POLE ARCS AND PERMEANCE SHAPE

Professor LAWRENSON et al. have defined the "feasible triangle" /8/ which determines the range and limits of pole arcs values β_s° and β_r° for stator and rotor.

Hence, it is preferable to choose β_r° greater than β_s° , this permits an increase of the winding area. To minimize unaligned permeance, it is necessary to respect the following condition :

$$\beta_s^\circ < \alpha_r^\circ - \beta_r^\circ$$

Figure 4 shows mechanic angles α_o° and α_c° corresponding to flat parts θ_{po} and θ_{pc} in linearized permeance shape (figure 1).

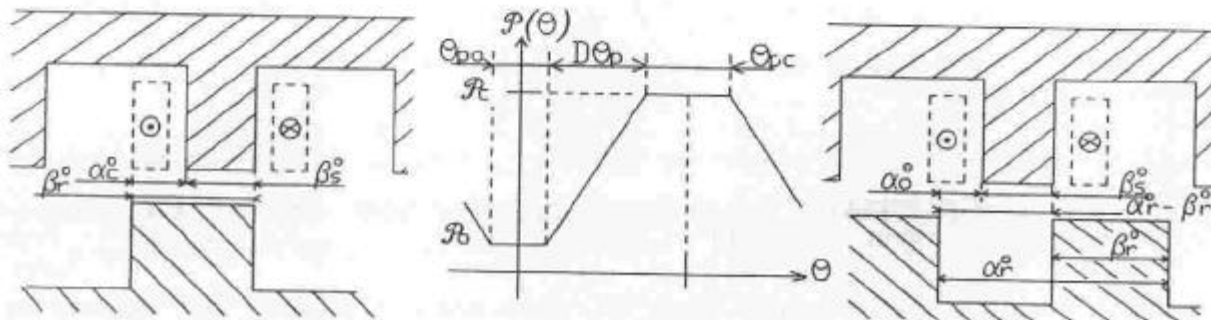


Figure -4-

Flat zones of permeance in aligned and unaligned positions

In these conditions, stator pole arc gives the value of $D\theta_p$ directly :

$$D\theta_p = 2\pi \cdot \beta_s \cdot \frac{N_r}{N_s} \quad [2.1]$$

Angles α_o° and α_c° can be written :

$$\alpha_o^\circ = \alpha_r^\circ - \beta_r^\circ - \beta_s^\circ$$

$$\alpha_c^\circ = \beta_r^\circ - \beta_s^\circ$$

So, rotor pole arc defines θ_{po} and θ_{pc} angles :

$$\theta_{po} = N_r \cdot \left[(1 - \beta_r) \cdot \frac{2\pi}{N_r} - \beta_s \cdot \frac{2\pi}{N_s} \right] \quad [2.2]$$

$$\theta_{pc} = N_r \cdot \left[\beta_r \cdot \frac{2\pi}{N_r} - \beta_s \cdot \frac{2\pi}{N_s} \right] \quad [2.3]$$

3- LINEARIZED MAGNETIC CHARACTERISTICS IN OPPOSITION AND CONJUNCTION - AVERAGE TORQUE COMPUTATION

Formulae [1.5, 1.6] showed that it was necessary to know permeances \mathcal{P}_o , \mathcal{P}_c and \mathcal{P}_s as well as saturation amperes-turns nIs . The model was intentionally simplified to permit better evaluation of dimensional parameters. Of course, a more sophisticated model would provide greater accuracy in predetermination.

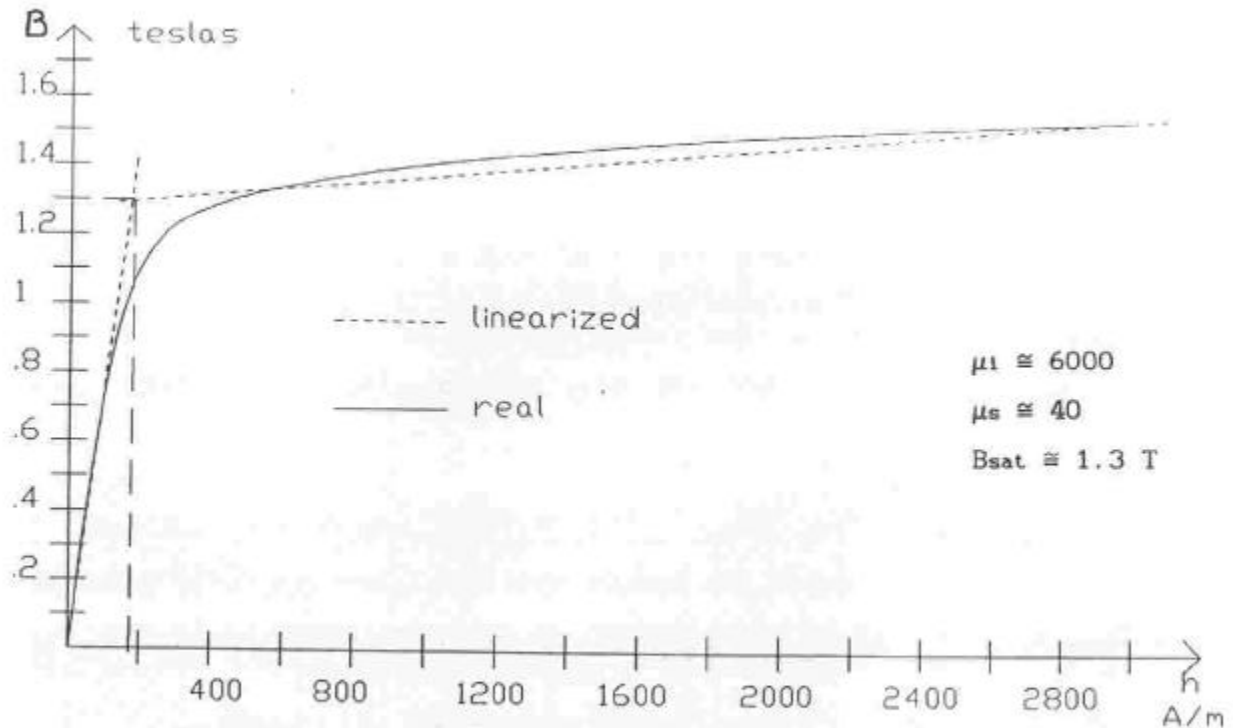


Figure -5-

Real and linearized magnetic material characteristics

In aligned position core saturation occurs, so we must take into account characteristic $b(h)$ of magnetic material. To have curve $\varphi(ni)$ consist of linear segments, $b(h)$ must be linearized : we defined two permeability slopes μ_1 and μ_s as shown in figure 5. The present motor is assembled with laminated steel UGINE NO 10 (0.1 mm thickness).

If we break up magnetic circuit into sections with constant areas regarding stator and rotor teeth and yoke, we can obtain from the various dimensions analytic expressions for permeances \mathcal{P}_c and \mathcal{P}_s . For the sake of clarity, we shall consider the particular case when the area of the whole magnetic circuit is constant and equal to that under a stator pole : S_F . Then we have :

$$\mathcal{P}_c = \frac{\mu_o . S_F}{\frac{l_F}{\mu_1} + 2 . e} \quad [3.1]$$

where : $S_F = 1 . \beta_s . \frac{2\pi . r}{N_s} . k_F$ [3.2]

k_F is the ratio of effective length to iron length of laminated stack (stack factor), and :

$$l_F \cong (2 + \pi) . (R_{ext} - \frac{e_c}{2}) \quad [3.3]$$

When magnetic circuit is saturated, permeance slope value is :

$$\mathcal{P}_s = \frac{\mu_o . S_F}{\frac{l_F}{\mu_s} + 2 . e} \quad [3.4]$$

and saturation limit is defined by :

$$nI_s = \frac{B_{sat}}{\mu_o} (\frac{l_F}{\mu_1} + 2 . e) \quad [3.5]$$

In the present example (with $k_F = 0.9$), numerical values are :

$$\underline{\mathcal{P}_c = 3.75 \mu H} \quad \underline{\mathcal{P}_s = 0.12 \mu H} \quad \underline{nI_s = 126 A}$$

Note : the value of μ_s must be determined in regard to the level of iron saturation ; then, at low saturation levels, μ_s is greater than at higher levels and the value of \mathcal{P}_s is greater too. Then, if $nI_M < 400 A$, we can have, in our example, $\mu_s \cong 80$ and $B_{sat} \cong 1.1 T$.

In unaligned position, we can calculate permeance with several methods /9, 10/. The solution proposed by Tormey, Torrey and Levin /10/ is particularly profitable : it is based on the finite elements method and requires knowledge of only two length ratios : rotor interpolar arc ($\alpha_r^\circ - \beta_r^\circ$) to stator pole arc (β_s°) and rotor interpolar arc length ($(\alpha_r^\circ - \beta_r^\circ) . r$) to rotor pole undercut (h_r).

In our particular case, we obtained :

$$\mathcal{P}_o = 0.3 \mu\text{H}$$

Figure 6 shows $\varphi(ni)$ curves in opposition and conjunction measured -- with 50 Hz sine wave supply by measuring current and integrating induced voltage in probe coil-- and linearized with our method. Chart I compares measured ($n = 40$ turns per phase) and computed values of linearized model :

		$\mathcal{P}_c/\mu\text{H}$	$\mathcal{P}_o/\mu\text{H}$	$\mathcal{P}_s/\mu\text{H}$	nI_s/A	φ_{sat} mWb
$nI_m < 400A$ $\mu_1=6000$ $\mu_s \cong 80, B_{sat} \cong 1.1 T$	measure	3.3	0.27	0.21	100	0.33
	computation	3.75	0.3	0.23	106	0.4
$nI_m < 1000A$ $\mu_1=6000$ $\mu_s \cong 40, B_{sat} \cong 1.3 T$	measure	3.3	0.27	0.11	120	0.4
	computation	3.75	0.3	0.12	126	0.47
$\mu_1=4000$ $\mu_s \cong 40, B_{sat} \cong 1.1 T$	computation	3.39	0.3	0.12	118	0.4

Chart I

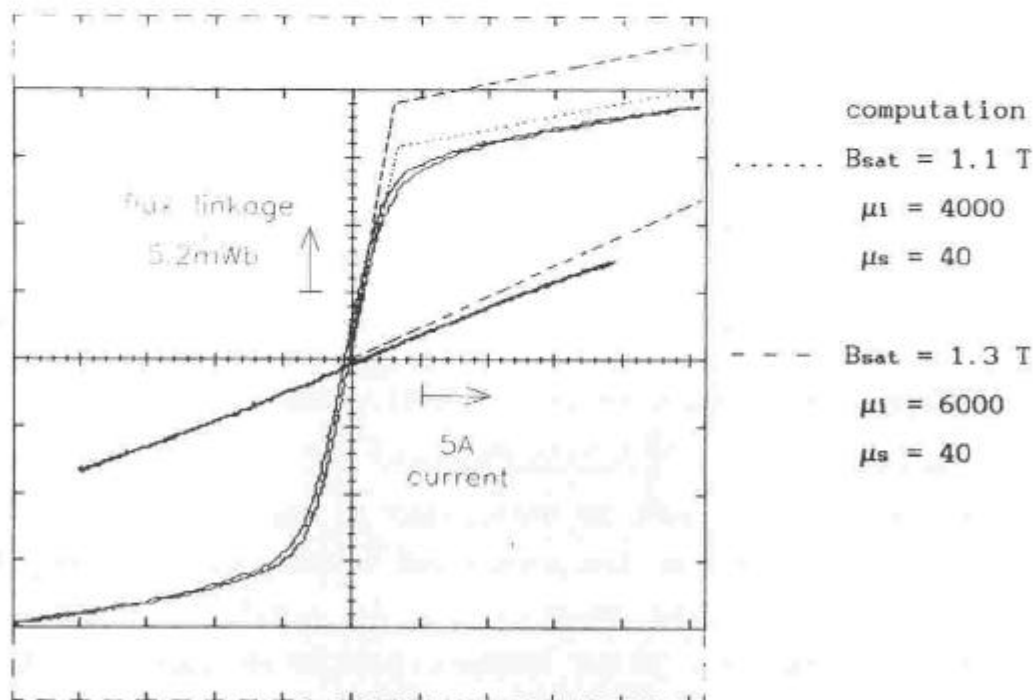


Figure -6-

Measured and calculated conjunction and opposition $\varphi(ni)$ curves

For our model to be satisfactory, smaller values had to be chosen for B_{sat} and μ . This must be due to the mechanical strength of the frame.

4- DETERMINATION OF POLE ARCS

The value of β_s is chosen in relation to torque pulsations. To achieve a regular torque with q phases, we can have :

$$D\theta_p = \frac{2\pi}{q} \quad [4.1]$$

In the case of 6-4 V.R.M., with [2.1, 4.1] : $\beta_s = 0.5$

The value of β_s influences permeances \mathcal{P}_c , \mathcal{P}_o , \mathcal{P}_s .

So winding area is proportional to $(1 - \beta_s)$, then copper losses - average torque ratio τ (or "torque per ampere") depends on β_s . A high value for β_s gives a greater flux in aligned position but requires a higher current density for given amperes-turns.

After choosing β_s , we can determine the value of β_r , this influences opposition permeance \mathcal{P}_o and permeance shape. In figure 7, these influences are shown in the case of our example of motor with $\beta_s = 0.5$.

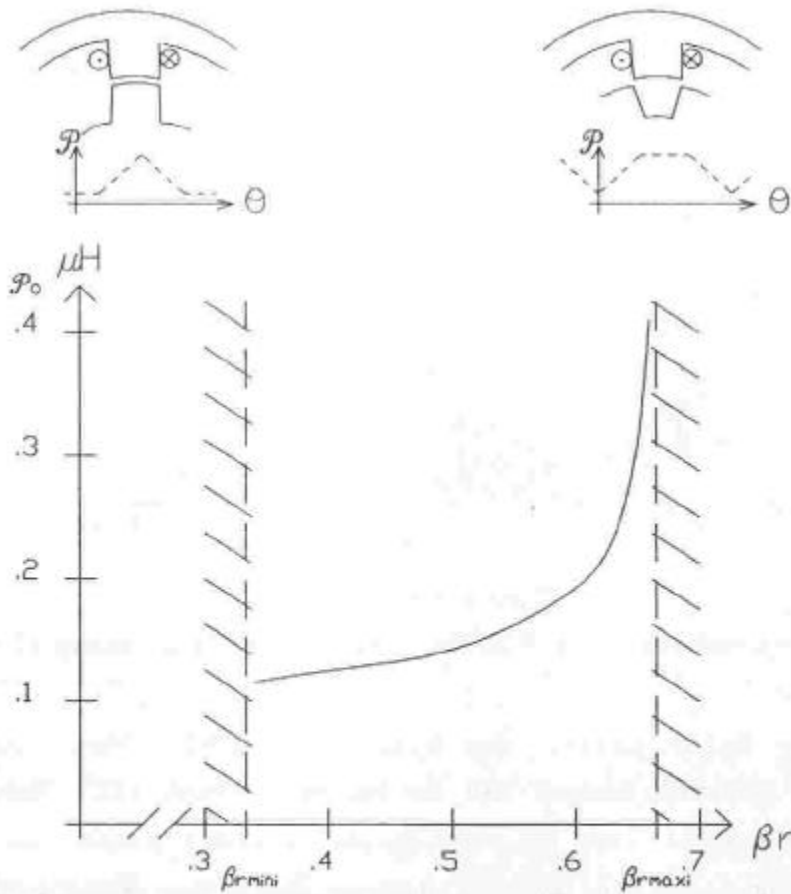


Figure -7-

β_r influence on unaligned permeance and permeance shape

The variation range of β_r^* is limited by $\beta_{r\text{minl}}^*$ and $\beta_{r\text{maxl}}^*$ (see §1) :

$$\beta_{r\text{maxl}}^* = \alpha_r^* - \beta_s^* \Rightarrow \beta_{r\text{maxl}} = 1 - \beta_s \cdot \frac{N_r}{N_s} \quad [4.2]$$

$$\beta_{r\text{minl}}^* = \beta_s^* \Rightarrow \beta_{r\text{minl}} = \beta_s \cdot \frac{N_r}{N_s} \quad [4.3]$$

Figure 8 describes V.R.M. basic converter (asymetrical half-bridge).

To switch on current, maximal available voltage is equal to :

$$U_{P\text{Max}} = U_0 - 2 \cdot \delta V_K \quad [4.4]$$

where U_0 is the D.C. voltage source supplying the converter.

To switch off current, maximal available negative voltage is :

$$U_{N\text{Max}} = U_0 - 2 \cdot \delta V_d \quad [4.5]$$

where δV_K and δV_d are voltage drops of switches K_1 K_2 and diodes D_1 D_2 . With medium voltages (greater than 100 V), voltage drops can be neglected. Between switching on and off, current is regulated by P.W.M.

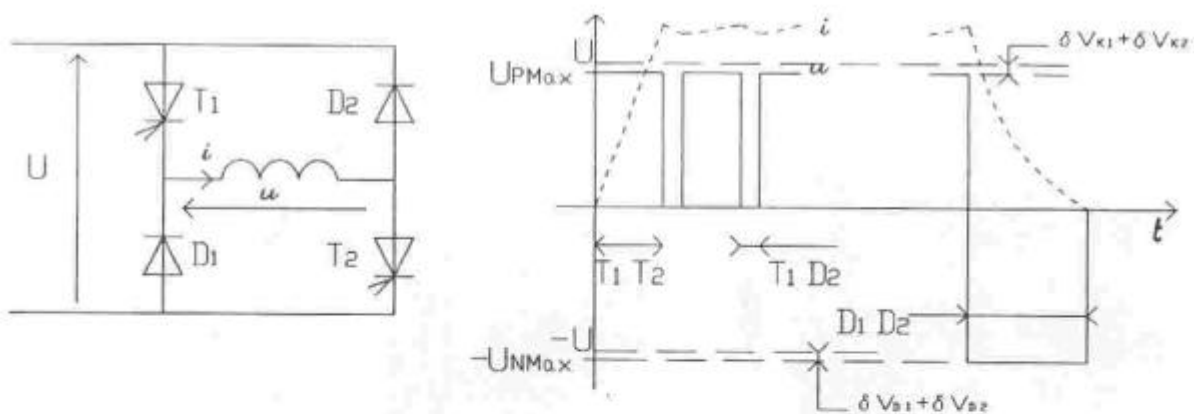


Figure -8-

One-phase basic converter for V.R.Ms. and maximum switching voltage

To maximize motor power, the highest possible base speed is required ; then nominal torque has to be maintained till that base speed has been reached. Then at base speed, current phase has to be switched on during angle θ_{po} and off during angle θ_{pc} . Figure 9 shows current and voltage in a phase at base speed ; we can see that current falls with two slopes and that saturation enhances quick switching. We can write (n is the number of turns for one phase) :

- in unaligned position, current rise time is equal to :

$$t_r = \frac{\theta_{po}}{\omega_b} = \frac{n^2 \cdot \mathcal{P}_o \cdot I_M}{U_{PM_{max}}}$$

So, electric angular speed is : $\omega = N_r \cdot \Omega$

Then :
$$\theta_{po} = \frac{n^2 \cdot \mathcal{P}_o \cdot N_r \cdot \Omega_b \cdot I_M}{U_{PM_{max}}} \quad [4.6]$$

where Ω_b is base angular speed and I_M current amplitude corresponding to required torque.

- in aligned position, with the same method, we obtained :

■ if $I_M \leq I_s$ (saturation current) :

$$\theta_{pc} = \frac{n^2 \cdot \mathcal{P}_c \cdot N_r \cdot \Omega_b \cdot I_M}{U_{NM_{max}}} \quad [4.7]$$

■ if $I_M > I_s$:

$$\theta_{pc} = \frac{n^2 \cdot N_r \cdot \Omega_b}{U_{NM_{max}}} \left[\mathcal{P}_c \cdot I_s + \mathcal{P}_s \cdot (I_M - I_s) \right] \quad [4.8]$$

or :

$$\theta_{pc} = \frac{n^2 \cdot N_r \cdot \Omega_b}{U_{NM_{max}}} \varphi(n I_M)$$

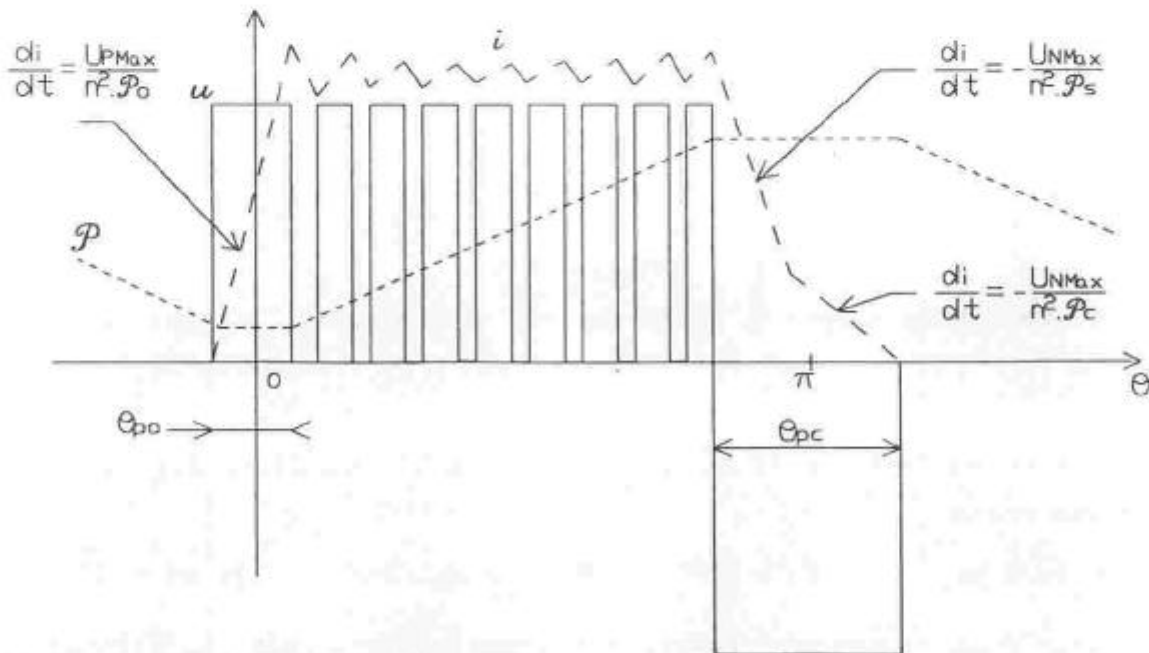


Figure -9-

Current and voltage waveforms at base speed

In the case of our motor, we measured switching times in opposition and conjunction and found that this calculation method is

accurate enough :

Figure 10 shows current oscillograms. We can see that measured current slopes are similar to computed di/dt , then voltage induced by mutual coupling can be neglected.

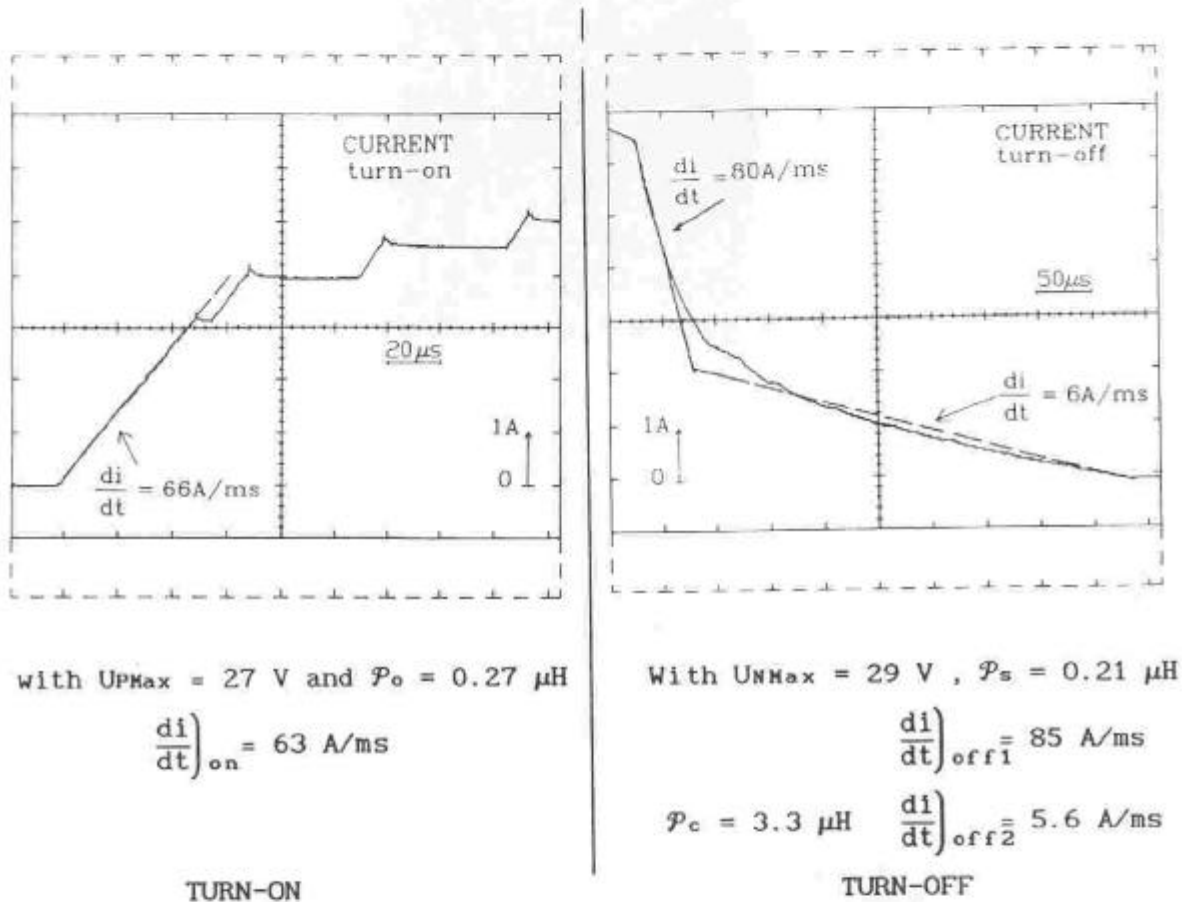


Figure -10-

Switching slopes of phase current with magnetic saturation

With expressions [2.2, 2.3], [4.2, 4.3] and [4.6, 4.7 or 4.8], we can write :

$$\blacksquare \text{ if } I_M \leq I_s \quad \mathcal{P}_o = \frac{\beta_{rmax1} - \beta_r}{\beta_r - \beta_{rmin1}} \frac{U_{PMax}}{U_{NMax}} \mathcal{P}_c \quad [4.9]$$

$$\blacksquare \text{ if } I_M > I_s \quad \mathcal{P}_o = \frac{\beta_{rmax1} - \beta_r}{\beta_r - \beta_{rmin1}} \frac{U_{PMax}}{U_{NMax}} \left[(\mathcal{P}_c - \mathcal{P}_s) \frac{nIM}{nI_s} + \mathcal{P}_s \right] \quad [4.10]$$

So, when taking into account both function \mathcal{P}_o versus β_r (§4, figure 7) and current value I_M , we can determine the optimal value for β_r which permits to maximize base speed Ω_b .

When the value of β_r has been determined, the number of turns n can be obtained with [4.7] for instance. Chart II gives, in the case of our motor, for various I_M values, average torque calculated with [1.4, 1.5, 1.6], for optimal value of β_r , number of turns n and "size power ratio" δ'' /5,6/ :

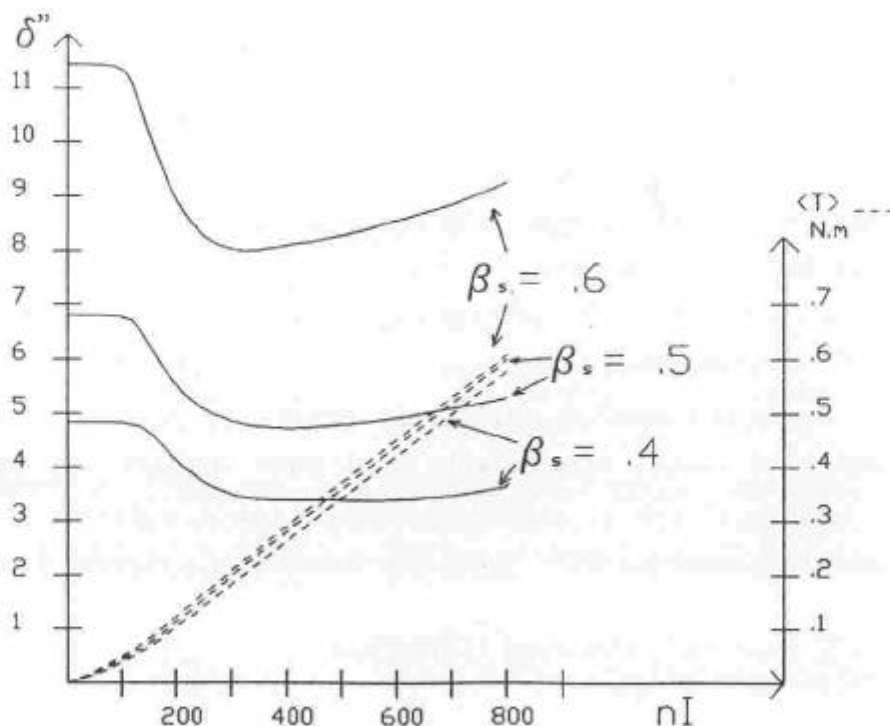
$$\delta'' = \frac{U_{Max} \cdot I_M}{\langle T \rangle \cdot \Omega} \cdot q \tag{4.11}$$

$n I_M / A$	100	200	300	400	500	600	700	800
β_r	.643	.635	.625	.617	.61	.603	.598	.593
$\mathcal{P}_o / \mu H$.267	.241	.22	.207	.199	.192	.187	.183
$\langle T \rangle / Nm$.033	.11	.2	.28	.36	.44	.52	.6
$n / turn$	71	53	51	49	46	45	42	41
δ''	6.8	5.3	4.8	4.7	4.8	4.9	5.1	5.3

V.R.M. 6-4 with $\beta_s = 0.5$, $U_{PMax1} = 27$ V, $U_{NMax1} = 29$ V at 5000 rpm

Chart II

S.P.R. defines required "silicium power" to supply motor at given power. Then, we can note the favourable influence of magnetic saturation on current switching capability of converter. S.P.R. can be reduced significantly.



β_s influence on Size Power Ratio and Torque

Figure -11-

If we reduce stator teeth angle -- hence decrease β_s -- switching angles θ_{po} and θ_{pc} can be increased. So, for example, with the same number of turns, the same voltage, the same current -- therefore the same torque -- speed can be increased and S.P.R. is improved. However torque becomes more pulsating. Figure 11 shows S.P.R. and average torque versus maximum amperes-turns nIM with three values for β_s .

5- CONCLUSIONS

With a model with simplified magnetic characteristics, we showed that we could optimize teeth angles to maximize maximum power of V.R.Ms. with a given converter and square wave current. Then, with permeance or inductance obtained waveforms, on one hand, we can product relatively low torque ripple with simple supply mode and low resolution shaft sensor on a large speed range or, on the other hand, it is easier to supply each phase with optimized current waveforms to have lower torque ripple, but with complexier control of current and higher resolution position sensor. We proposed a method to achieve this optimization with as few parameters as possible. But a continuous model for the iron magnetic characteristic could help increase computation accuracy /12, 13/.

As the choice of β_s is, essentially, guided by pulsating torque constraints, we showed that the choice of β_r is determined by current switching, hence by maximum average torque. Magnetic saturation is highly profitable to increase power. It is known that a small airgap allows an increase in torque at given copper losses /7/, but it is profitable for the converter too. A diminution in stator angle allows to increase convertible power with a given converter, but that means an increase in ripple torque.

In practice, at high saturation levels, permeance shape gets distorted, particularly, θ_{pc} angle (flat part in conjunction) increases. So we can advance switch-off angle.

Beyond base speed, supply with full wave voltage and control of switching angles allows to increase maximum power and extend constant power operating zone/8, 11/. But, in this case, ripple torque will increase.

REFERENCES

- 1 P. J. LAWRENSON : "Switched Reluctance Motor Drives", *Electronics & Power*, February 1983, pp. 144-147.
- 2 T. J. E. MILLER : "Brushless Permanent Magnet and Reluctance Motor Drives", Oxford Science Publications 1989, pp. 147-191.
- 3 A. MAILFERT : "Machines à réluctance variable", *Techniques de l'Ingénieur D550*, mars 1986.
- 4 C. GLAIZE : "Recherche des formes optimales d'alimentation des machines à réluctance variable", *Rev. Phys. Appl.* 20, pp. 769-794, novembre 1985.
- 5 B. MULTON, C. GLAIZE : "Optimisation du dimensionnement des alimentations des machines à réluctance variable", *Rev. Phys. Appl.* 22, pp. 339-357, mai 1987.
- 6 B. MULTON, C. GLAIZE "Size Power Ratio Optimization for the Converters of Switched Reluctance Motors", IMACS TC'1, September 1990.
- 7 B. MULTON, D. BONOT, J. M. HUBE, "Conception d'un moteur à réluctance autocommuté alimenté en courant", MOPP Lausanne, juillet 1990.
- 8 LAWRENSON, P. J., STEPHENSON, J. M., BLENKINSOP, P. T., CORDA, J. and FULTON, N. N. : "Variable Speed Switched Reluctance Motors", *IEE Proc. B, Elect. Power Appl.*, vol.127, pp. 253-265, July 1980.
- 9 J. CORDA, J. M. STEPHENSON : "Analytical Estimation of the Minimum and Maximum Inductances of a Double-Salient Motor", *proc. IEE*, Vol.126, May 1979.
- 10 D. P. TORMEY, D. A. TORREY, P. L. LEVIN : "Minimum Airgap-Permeance Data for the Doubly-Slotted Pole Structures Common in Variable-Reluctance -Motors", *proc. IEEE*, Seattle Sept. 1990, pp. 196-200.
- 11 B. K. BOSE, T. J. E. MILLER, P. M. SZCZESNY, W. H. BICKNELL : "Microcomputer Control of Switched Reluctance Motor", *IEEE Vol I. A.-22* n°4 July-August 1986 pp.708-715.
- 12 A. R. EASTHAM, H. YUAN, G. E. DAWSON, P. C. CHOUDHURY, P. M. CUSACK : "A Finite Element Evaluation of Pole Shaping in Switched Reluctance Motors", *ELECTROSOFT 1990*, Vol.1, N°1, pp.55-67.
- 13 M. MOALLEM, C. M. ONG, L. E. UNNEWEHR : "Effect of Rotor Profiles on the Torque of a switched Reluctance Motor", IAS, IEEE Conf., Seattle 1990, pp.247-253.

Manuscript received in final form October 21, 1992
Request reprints from B. Multon